International Journal for Housing Science and Its Applications
Publish August 10, 2025. Volume 46, Issue 4 Pages 103-116

https://doi.org/10.70517/ijhsa46408

Research on power balance calculation of flexible resources based on adaptive genetic algorithm in smart grid framework

Xuezheng Ying[1,*], Weidong Zhu[1], Dongdong Ying[1], Yuyi Lou[1] and Xingxing Zhou[2]
[1] Hangzhou Electric Power Design Institute Co., LTD., Hangzhou, Zhejiang, 310012, China
[2] Chongqing Xingneng Electric Co., LTD., Chongqing, 400039, China
Corresponding authors: (e-mail: 15696198698@163.com).

Abstract Grid planning plays an important role in the long-term development of electric power enterprises, is an important part of the national economy and social development, and plays a fundamental role in supporting the development of the whole country. In this paper, the day-ahead-intraday scheduling model is constructed with the objective of integrated energy system operation cost and the coordinated optimization of integrated flexible loads, cogeneration units and wind power from the perspective of multi-timescale scheduling. The genetic algorithm is improved based on the concept of adaptive, and the improved adaptive genetic algorithm is used to solve the system. The optimization model is verified to be effective for both load adjustment and small load fluctuation through examples, while the improved adaptive genetic algorithm can be effectively applied to the integrated energy system optimization and operation problem, and the proposed multi-timescale optimization and operation scheme has the advantages of reducing the operation cost and improving the consumption of renewable energy.

Index Terms integrated energy system, multi-timescale, adaptive genetic algorithm, load fluctuation

I. Introduction

Smart grid, as a new type of energy system, aims to realize efficient, stable and sustainable supply of electricity by combining intelligent technology with power system, in which power balance calculation, as an important part of smart grid, has received wide attention [1], [2].

Power balance refers to the balance between power supply and demand, which is an important root and link in power system planning and system design, and it is also necessary to progress the power balance calculation in the feasibility study, access system and preliminary design stages of power supply engineering and transmission and transformation engineering [3]-[6]. In fact, the establishment of any planning model or the formation of any planning scheme involves power balance analysis [7]. The calculation of power balance is likewise an important part of the work when preparing the near-term plan of the power system [8]. Power balance is actually the study of the relationship between supply and demand of the power system, that is, to make the power system in the planning period, the system needs to send and generate the maximum load and the system has the production capacity of generating equipment balanced [9]-[11]. The purpose of this balance is to make the power system in the planning period, in a more reasonable structure and way to carry out the production and transmission of electricity, and to meet the growing demand for electricity load [12], [13]. How to fulfill this balance and meet the needs of the system is the task of power balancing and power planning [14]. Generally speaking, the power balance requirements are carried out year by year, not only because the annual power load is fluctuating and changing, but also the actual output of each power plant of the system is different every year, so the year-by-year balance analysis is conducive to carry out the correction and review of the power supply construction, and at the same time, it also provides a basis for the direction of the next stage of the whole system planning [15]-[18].

Considering the multi-timescale characteristics of grid load response and response cost, the study establishes a multi-timescale optimal scheduling model considering the integrated flexible load response, and coordinates and optimizes flexible loads, cogeneration units and wind power from the perspective of multi-timescale scheduling. Adaptive improvements are made to address the problems of prematurity, slow convergence, low accuracy and difficulty in solving the nonlinear equation constraints in the model that occur in the solution process of traditional GA algorithms. Finally, the proposed optimized operation model is solved by setting different operation scenarios through specific examples, and the results are compared and analyzed.

II. Flexible Resource Power Balance Dispatch Model in the Smart Grid Framework

II. A. Smart Grid Flexible Resource Power Balancing

Smart grid load and storage integration balance is based on load forecasting, comprehensively considering the source network load and storage and other aspects of the flexible resources involved in power balance, to get the calculated load, on the basis of which the grid planning.

II. A. 1) Integrated energy system architecture

Comprehensive energy systems generally use natural gas as the primary energy source, heat and electricity as the main energy sources, and the system contains various types of energy production, conversion and storage equipment to meet the demand for multiple loads on the user side. The specific system architecture of the gas steam combined cycle unit is shown in Figure 1.

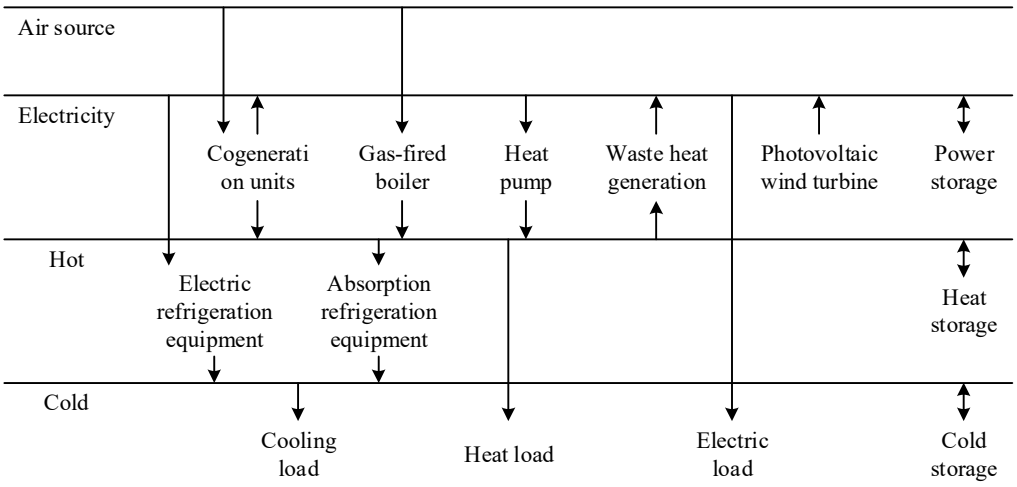

Figure 1: Integrated energy system architecture

II. A. 2) Optimized scheduling architecture for integrated energy systems

Day-ahead scheduling accuracy is low, and it is difficult to use the day-ahead scheduling strategy alone to give good play to the multi-timescale characteristics of the flexible load response; at the same time, as the energy system shifts from day-ahead scheduling to intraday scheduling and the accuracy of the prediction curves of renewable energy power generation improves, the accuracy of the day-ahead scheduling is too low to apply to the change of the accuracy of the day-ahead shifting to the intraday. Therefore, it is necessary to establish a multi-timescale optimal scheduling model to reasonably coordinate various types of flexible loads.

Aiming at the above problems, this paper proposes a joint day-ahead-intraday optimal scheduling architecture. The multi-scale optimal scheduling study of integrated energy system considering flexible load response is divided into two main parts according to time scales: pre-day long time scale optimal scheduling and intra-day short time optimal scheduling. Within the day-ahead long time-scale optimal scheduling, thermal and electric flexible loads are divided into day-ahead curtailable thermal and electric loads, transferable thermal and electric loads, and leveling thermal and electric loads; within the intraday short time-scale optimal scheduling, taking into account the day-ahead scheduling plan, the amount of intraday load changes, renewable energy output, and not affecting the user's production, etc., the intraday secondary adjustment of the loads is only considered for the participation of the day-ahead curtailable thermal and electric loads. Dispatch.

II. B. Multi-time scale flexible resource power balance optimization operation model

II. B. 1) Multi-scale optimized scheduling process

Multi-timescale integrated energy optimization scheduling is divided into two major parts: day-ahead and intra-day. Day-ahead optimal scheduling first determines whether the day-ahead scheduling cycle is reached, and if so, inputs the day-ahead forecast load data and solves the day-ahead scheduling model, and determines the day-ahead scheduling plan containing the day-ahead curtailment amount, transferable amount, and leveling amount; day-ahead optimal scheduling first determines whether the day-ahead scheduling cycle is reached, and if so, inputs the day-ahead scheduling based on the 2-h advance of the integrated energy system in the wind power, PV If it is reached, the forecast value of wind power and photovoltaic in the integrated energy system and the system

adjustment amount are inputted 2h in advance on the basis of the day-ahead scheduling and the intra-day scheduling model is solved to form the intra-day scheduling plan which includes the load reduction amount in the day-ahead.

II. B. 2) Day-ahead scheduling model

(1) Objective function

The objective is to minimize the sum of system unit generation, startup and shutdown costs, steam production costs and flexible load dispatch costs:

$$\min E = \min\left[\sum_{t\in T}\left(\sum_{i\in Z} C_{t,i}^{dr} + \sum_{i\in Z} C_{t,i}^{OF} + E_{t,i} + O_{t,i}^{en} + O_{t,i}^{tr} + C_{dl}\right)\right] \tag{1}$$

$$C_{fl} = C_{xue} + C_{ping} + C_{zhuan} \tag{2}$$

$$C_{xue} = M_{xue} \cdot p_{xue} \cdot \Delta t \tag{3}$$

$$C_{ping} = M_{ping} \cdot S_{ping} \cdot F_{on1} \tag{4}$$

$$C_{zhuan} = M_{zhuan} \cdot S_{zhuan} \cdot F_{on2} \tag{5}$$

where, E is the expected overall system cost; t is one of the time periods in the dispatch cycle; Z is the set of units; $C_{t,i}$ is the unit's i combustion cost; $C_{t,i}^{oF}$ is the unit's i operating cost; $E_{t,i}$ is the cost incurred by the system from trading with the larger grid; $O_{t,i}^{en}$ is the revenue of the unit producing steam; $C_{t,i}^{tr}$ is the transmission cost of steam; C_n is the flexible load dispatch cost; C_{xue} is the curtailable load cost; C_{ping} is the levelized load cost; and C_{zhuan} is the transferable load cost; M_{xue} is the compensation for the unit capacity of the curtailable load; p_{xue} is the power of the curtailable unit; M_{ping} is the compensation for the unit capacity of the leveled load; S_{ping} is the capacity of the leveled load; and F_{on1} is the system judgment leveling command, which has only two 0 and 1 state. F_{on2} is the system judgment transfer instruction, only 0 and 1 two states.

(2) System power balance constraints

$$\sum_{t\in T}\left[\sum_{i\in Z} e_{i,t,s}^{grn} - e_{i,t,s}^{con} + e_{i,s}^{b}\right] = \sum_{t\in T} D_i^e \tag{6}$$

$$e_{t,s}^{b} = e_{t,s}^{buy} - e_{t,s}^{sell} \tag{7}$$

where, $e_{i,t,s}^{gen}$ is the amount of electricity produced by the production unit; $e_{i,t,s}^{con}$ is the amount of electricity consumed by the system itself; and $e_{t,s}^{b}$ is the change in electricity generated by the large grid transaction; $e_{t,s}^{buy}$ is the amount of electricity bought from the large grid; $e_{t,s}^{sell}$ is the amount of electricity sold to the large grid; and D_t^e is the amount of system electrical load at time t.

(3) System heat balance constraints

$$\sum_{t\in T}(G_{t,s} + L_{t,s} + \sum_{i\in Z} h_{i,t,s}^{gen} + G_{i,s}^{c}) = \sum_{t\in T} D_t^h \tag{8}$$

$$G_{t,s} = A_{t,s} + P_{t,s} \tag{9}$$

where, $h_{i,t,s}^{gen}$ is the unit steam production; $G_{t,s}$ is the overall steam storage in the system at time t; D_i^h is the heat load of the system at time t; $L_{t,s}$ is the loss of steam during transmission; $A_{t,s}$ is the steam storage in pipeline at time t in the steam storage; $P_{t,s}$ is the steam storage in the pipeline at time t; and $G_{t,s}^{c}$ is the steam consumption in the system.

(4) Unit start-stop constraints

$$\begin{cases} \Delta z_{i,t,s} \geq z_{i,t,s} - z_{i,t-1,s} \\ \Delta z_{i,t,s} \leq 1 - z_{i,t-1,s} \\ \Delta z_{i,t,s} \leq z_{i,t-1,s} \\ \sum_{t\in T} \Delta z_{i,t,s} \leq N_{i,s} \end{cases} \tag{10}$$

where, $\Delta z_{i,t,s}$ is the variation of unit start/stop; $z_{i,t,s}$ is the unit start/stop state, which is divided into the binary state of 0, 1; $N_{i,s}$ is the maximum amount of unit turn-on allowed in the system.

II. B. 3) Intraday scheduling model

(1) Objective function

The day-ahead scheduling strategy has some limitations. Firstly, the time scale is long, which cannot be better adjusted according to the actual load changes; secondly, there will be some deviation between the system operation and load demand changes under the day-ahead scheduling strategy. Therefore, it is necessary to add the intraday scheduling strategy to the day-ahead scheduling to shorten the time scale to reduce the deviation. The optimization objectives of the intraday scheduling strategy and the day-ahead scheduling strategy are the same, both of which are to minimize the system operation cost. The objective function can be expressed as:

$$\min E = \min\left[\sum_{t\in T}\left(\sum_{i\in Z} C_{t,i}^{be} + \sum_{i\in Z} C_{t,i}^{OF} + E_{t,i} + O_{t,i}^{en} + C_{xue,lh}\right)\right] \tag{11}$$

where, E is the expected overall system cost; Z is the set of units; $C_{t,i}^{be}$ is the combustion cost of unit i; $C_{t,i}^{OF}$ is the operating cost of the unit; $E_{t,i}$ is the cost incurred by trading the system and the larger grid; $O_{t,i}^{en}$ is the return on the steam production of unit i; $C_{xue,lh}$ is the intraday cost of available load curtailment.

(2) System power balance constraints

$$\sum_{i\in T}\left[\sum_{i\in Z}(e_{i,t,s}^{gen} - e_{i,t,s}^{cen}) + e_{t,s}^{b} + e_{t,s}^{c}\right] = \sum_{i\in T} D_{t}^{c} \tag{12}$$

where, $e_{i,t,s}^{gen}$ is the amount of electricity produced by the production units; $e_{i,t,s}^{con}$ is the amount of electricity consumed by the system itself; $e_{t,s}^{b}$ is the change in the amount of electricity generated by the large grid transactions; $e_{t,s}^{c}$ is the change in the amount of electricity generated by the electricity storage devices within the system; and D_{t}^{e} is the amount of electricity loaded into the system at time t the amount of electrical load of the system.

(3) System heat balance constraints

$$\sum_{t\in T}(G_{t,s} + G_{t,s}^{c} + \sum_{i\in Z} h_{i,t,s}^{gen}) = \sum_{i\in T} D_{t}^{h} \tag{13}$$

where, $h_{i,t,s}^{gen}$ is the unit steam production; $G_{t,s}$ is the overall steam storage in the system at time t; D_{i}^{h} is the system heat load at time t; and $G_{t,s}^{c}$ is the steam consumption in the system.

(4) Unit start-stop constraints

Since the time scale of the unit start-stop state change is long, the unit start-stop state cannot be optimized twice in the intraday short time scale scheduling plan, and the unit start-stop state of the previous day's scheduling plan is followed in the intraday scheduling plan.

(5) Flexible load constraints

$$p_{xue,lh}^{\min} \le p_{xue,lh} \le p_{xue,lh}^{\max} \tag{14}$$

where, $p_{xue,lh}^{\max}$ is the maximum power that can be cut during the day; $p_{xue,lh}^{\min}$ is the minimum power that can be cut during the day.

II. C. Model Solution Methods

II. C. 1) Genetic algorithms

Genetic Algorithm (GA) is an evolutionary algorithm that mimics the Darwinian evolutionary law of “natural selection” [19]. The GA algorithm first encodes the decision variables in the optimization problem as chromosomes (individuals), calculates the fitness of different individuals in the population, and then employs an iterative approach to perform selection, crossover, and mutation operator operations on the population to enable the population to evolve to generate a new subgeneration of the population, and ultimately generates the chromosomes that meet the optimization objective.

II. C. 2) Improving adaptive genetic algorithms

Traditional genetic algorithms use fixed crossover probabilities: and mutation probabilities without considering the differences in fitness between different individuals, resulting in the fact that individuals with larger fitness cannot be effectively retained, and those with smaller fitness cannot be given more chances to evolve, which largely restricts the convergence efficiency and convergence effect of genetic algorithms [20]. For this reason, an adaptive genetic algorithm that enables the values of P_t and P_m to be adaptively adjusted according to the size of individual fitness is proposed. The crossover and genetic probability formulas in its algorithm are as follows:

$$P_c = \begin{cases} \dfrac{P_{c1}(f_{\max} - f)}{f_{\max} - f_{\min}} & f \geq f_{avg} \\ P_{c2} & f < f_{avg} \end{cases} \tag{15}$$

$$P_m = \begin{cases} \dfrac{P_{m1}(f_{\max} - f')}{f_{\max} - f_{\min}} & f' \geq f_{avg} \\ P_{m2} & f' < f_{avg} \end{cases} \tag{16}$$

where f is the larger fitness value of the two parent individuals performing the crossover operation: f' is the fitness value of the parent individual performing the variation operation; $f_{\max}, f_{\min}$ and f_{avg} are the fitness maxima and minima of the individuals in the population and the mean values. $P_{c1}, P_{c2}, P_{m1}, P_{m2}$ are the crossover and variation parameters set during the solution process, $P_{c1}, P_{c2}, P_{m1}, P_{m2} \in (0,1)$.

However, the algorithm still has defects, for the individual with the largest or near-maximum fitness in the population, the values of P_c and P_m are close to 0, which will lead to the fact that the better individual cannot evolve in the: population at the early stage of the evolution, and thus the model is trapped in a locally optimal solution. The algorithm is further improved based on this algorithm by Ren Ziwu et al:

$$P_c = \begin{cases} P_{c1} - \dfrac{(P_{c1} - P_{c2})(f - f_{avg})}{f_{\max} - f_{avg}} & f \geq f_{avg} \\ P_{c1} & f < f_{avg} \end{cases} \tag{17}$$

$$P_m = \begin{cases} P_{m1} - \dfrac{(P_{m1} - P_{m2})(f - f_{avg})}{f_{\max} - f_{avg}} & f' \geq f_{avg} \\ P_{m1} & f' < f_{avg} \end{cases} \tag{18}$$

The improved GA algorithm can keep the good individuals evolved throughout the iteration process by raising the lower bounds of crossover and mutation probabilities of the individuals with the largest or nearly largest fitness in the population to P_{c2} and P_{m2}, respectively, which prevents the algorithm from falling into a local optimal solution and enhances the ability of global optimality search.

Improving the initial population generation method will make the model solution time too long and the computational efficiency is low; while the traditional method of constructing the penalty function usually adopts infinity or a very large fixed value as the penalty value, which will cause almost all the individuals in the population to obtain the same penalty value, so that their fitness value tends to be the same, resulting in the algorithm losing the direction of evolution. In addition, an unreasonable penalty function will also lead to problems such as reduced computational accuracy, inability to converge, or the penalty function is too sensitive to the parameters. Therefore, how to set an effective penalty function becomes the key to deal with constrained models with nonlinear equations. In this study, a new penalty function is constructed based on the distance relationship between the solution and the feasible domain.

For the nonlinear planning problem, the general model structure is as follows:

Objective function:

$$\min f(x) = f(x_1, x_2, \cdots, x_n) \tag{19}$$

$$\begin{cases} g_i(x) \leq 0, i = 1,2,3... \\ h_j(x) = 0, j = 1,2,3... \end{cases} \tag{20}$$

It is now defined that $d(x,Q)$ is the distance between the individual x in the population that exceeds the constraint the most and the feasible domain Q, which is given by the following formula:

$$d(x,Q) = \max\{0, g_{\max}(x), h_{\max}(x)\} \tag{21}$$

Among them:

$$\begin{aligned} g_{\max}(x) &= \max\{g_i(x), i = 1,2,...,m_1\} \\ h_{\max}(x) &= \max\{h_j(x), j = 1,2,...,m_2\} \end{aligned} \tag{22}$$

It can be seen that $d(x,Q) = 0$ when the point x is inside the definition domain Q; $d(x,Q) > 0$ when x is outside the definition and Q, and the larger $d(x,Q)$ is, it means that more than the point x is farther away from the feasible domain Q.

Meanwhile, define $FD(x)$ as the non-feasible point feasibility, which is given by the following formula:

$$FD(x)=\frac{\sum_{i=1}^{m_1}\gamma_i(x)+\sum_{j=1}^{m_2}\lambda_j(x)}{m_1+m_2} \tag{23}$$

$$\gamma_i=\begin{cases}1 & g_t(x)\le 0\\ 1-\dfrac{g_t(x)}{g_{\max}(x)} & 0<g_t(x)\le g_{\max}(x)\end{cases} \tag{24}$$

Among them:

$$\lambda_i(x)=\begin{cases}1 & h_j(x)=0\\ 1-\dfrac{|h_j(x)|}{h_{\max}(x)} & h_j(x)\ne 0\end{cases} \tag{25}$$

The $FD(x)$ also reflects the relationship between x and the feasible domain Q, $FD(x)\in[0,1]$. When the point x is within the domain of definition Q, $FD(x)=1$; when the point x is farthest from the feasible domain Q, $FD(x)=0$. It can be seen that the smaller $FD(x)$ is, the greater the degree of the individual breaking out of the constraint.

From the above two definitions, for the minimization objective, the new penalty function is constructed as follows:

$$eval(x)=\begin{cases}f(x) & x\in Q\\ \dfrac{f(x)}{(d(x,Q)+1/(FD+\alpha))^p} & f(x)<0, x\notin Q\\ f(x)*(d(x,Q)+1/(FD+\alpha))^p & f\ge 0, x\notin Q\end{cases} \tag{26}$$

where p and α are parameters satisfying $p\ge 1$ and $\alpha>0$. In this way, when x is in the feasible domain Q, the value of $eval(x)$ is equal to the value of the objective function; when x is not in the feasible domain Q, different degrees of punishment by the distance of the point x from the definition of the domain Q (the degree of breaking through the constraints) is changed, so as to make all the individuals in the population to the definition of the domain of the direction of evolution.

III. Analysis of examples

III. A. Base data for the algorithm

The energy input in this section includes the purchase of electricity from the higher power grid, the purchase of natural gas and wind power from the higher gas grid; the energy conversion and storage equipment includes cogeneration, electric boiler, electric-to-gas equipment, gas boiler, and electric, heat and gas storage equipment; and the load side includes the electric load, heat load and gas load.

Due to the northern winter wind abandonment, abandonment of light phenomenon is obvious, cogeneration units to provide thermal energy at the same time to increase the power output, resulting in more difficult to consume wind turbine power generation and photovoltaic power generation, so this example of the calculations in the winter of China's northern part of a typical integrated energy system as an example. The number of scheduling hours is T=24, and the price of natural gas is 3.5 yuan/m3, which is converted into a unit calorific value price of 0.37 yuan/(kW.h). The parameters of the energy supply equipment unit are shown in Table 1, and the parameters of the energy storage equipment unit are shown in Table 2, in which the system includes two CHP units with output power upper and lower limits of 2000kW and 100kW respectively. The forecast curves of typical Nippon, heat and gas loads are shown in Figure 2, and the forecast output curves of wind turbine and photovoltaic are shown in Figure 3. The purchased and sold electricity prices for each time period are shown in Table 3. Set R=300, M=100, L=60 in the fireworks algorithm.

Table 1: The system installed capacity and operation and maintenance coefficient

Type	Lower power /kW	Power limit /kW	Ci/(yuan/kW h)	Type	Lower power /kW	Power limit /kW	Ci/(yuan/kW h)
CHP	210	4200	0.0857	P2G	0	155	0.0715
WT	0	1200	0.0199	GB	0	650	0.0315
PV	0	400	0.0238	And electricity	-1200	4500	-
EB	0	900	0.0164	Gas purchase	-	5500	0.37

Table 2: Unit parameters of energy storage equipment

Type	Maximum capacity	$p_{c,j}^{\max}$	$p_{f,j}^{\max}$	Ci/(yuan/kW h)
ES	550Kw.h	100kW	100kW	0.015
HS	1200kW.h	420 kW	220kW	0.029
GS	420m3	220m3	70m3	0.035

Table 3: The price of electricity purchased and sold in each period

Section	Time period	Purchase electricity /(yuan/ (kW.h))	Power selling /(yuan/ (kW.h))
Peak time	08:00-11:00;17:00-22:00	0.95	0.75
Normal segment	07:00-08:00;11:00-17:00;22:00-23:00	0.55	0.43
Valley time	23:00-07:00	0.21	0.15

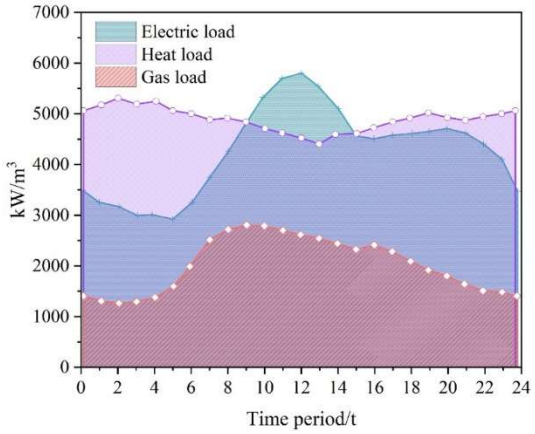

Figure 2: Electric load, heat load and gas load forecasting curve

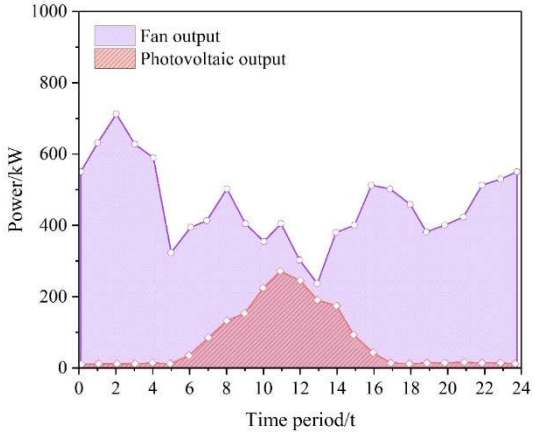

Figure 3: Predicted output curve of wind turbine and photovoltaic

III. B. Day-ahead and intraday scheduling analysis based on event mechanism

The day-ahead and intraday scheduling results of the integrated energy system obtained from this paper's simulation under a typical day in winter are shown in Fig. 4. The hourly average power of the original load curve of the day's load is used as the load forecast data for the day-ahead scheduling. The hotel welcomes unplanned occupancy at 14:00 on the day of operation, and the system receives the information and introduces a load adjustment event, which adjusts the heat load forecast on request, and a new operation plan is obtained from the intraday scheduling. Additional heat is deposited into the heat storage tank. By about 12:00 the gas turbine starts to run at full load. At this time, due to the increase in cooling and electrical loads, the system has to purchase power from the grid to satisfy the plant power and electrical loads. Around 14:00 a load adjustment event is generated, and the load side demand for heat loads is increased, so the heat pump machine output is increased in the subsequent intraday dispatch, and there is energy storage to match the output.

In the day-ahead scheduling plan, the system gives priority to the gas turbine for power generation, and the waste heat generated in the process is transferred to the lithium bromide unit for heat production, and the remaining heat load is provided by the heat pump unit. The centrifugal unit meets the cooling load demand by consuming electrical energy, and if the gas turbine power is not enough to meet the electrical load with the gas turbine consumption, the power is purchased from the grid. Figures 4(a) and (b) show the operation status of the gas turbine, heat pump unit and lithium bromide unit in the day-ahead scheduling plan and intra-day scheduling plan, respectively. The cooling load in the pre-day period is not high, the gas turbine does not need to be fully loaded, and there is extra heat energy stored in the heat storage tank. The gas turbine starts to run at full load at about 12:00. At this time, due to the increase in cooling and electrical loads, the system has to purchase power from the grid to satisfy the plant power and electrical loads. Around 14:00, a load adjustment event occurs, and the load side's demand for heat loads increases, so the heat pump output is increased in the subsequent intraday scheduling, and the energy storage is used to match the output.

Figure 4(c) shows the output schedule of the heat storage tanks on the operating day, and it is easy to know that due to the increase in heat load, the intraday scheduling increases the output power of the energy storage in the subsequent hours, and increases the heat output in the evening hours to heat up the energy storage. Figure 4(d) shows the purchased gas and purchased power of the system on the day. Comparing with the day-ahead scheduling, the intraday scheduling reprograms the heat output of the heat pump unit and the thermal storage when the event is generated. If the load is adjusted to continue to operate according to the previous day's schedule, the system has the choice of either backfiring the lithium bromide unit or releasing heat from the storage to fill the gap when the power shortage occurs. The energy efficiency of the lithium bromide unit is extremely low, which increases the energy cost of the system, and there is a limitation on the power of heat release by energy storage, so it is not possible to make up for the shortfall completely.

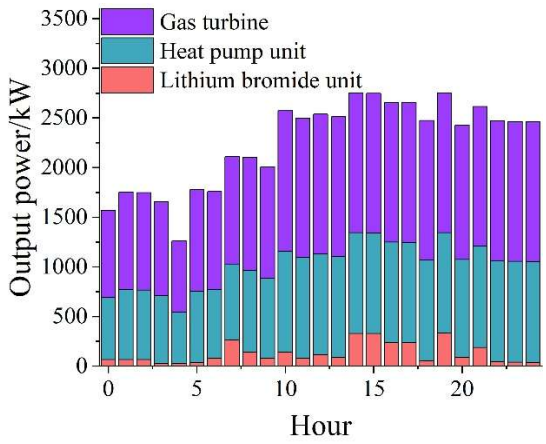

(a) Pre-schedule

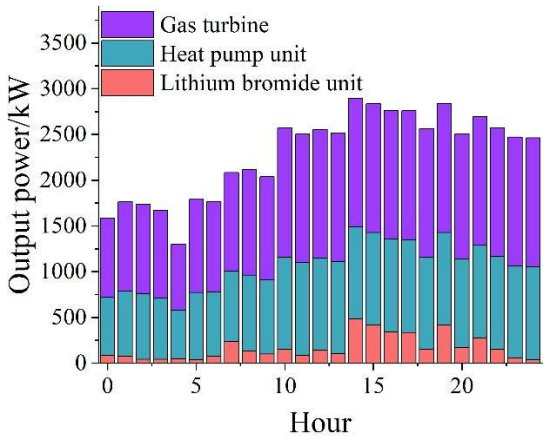

(b) Day dispatch

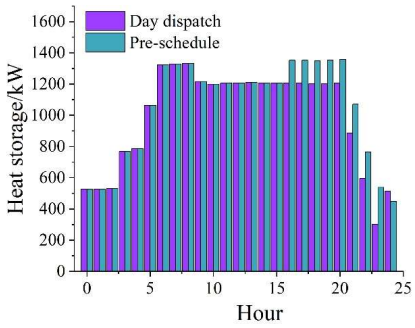

(c) Energy storage

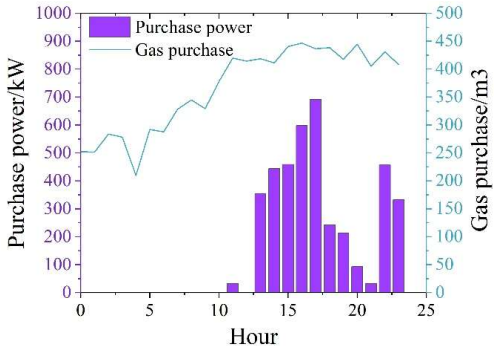

(d) Purchase electricity /Gas results

Figure 4: Day-ahead and intra-day scheduling results

The analysis shows that the role of day-ahead scheduling is to correct the difference between day-ahead scheduling and the actual operating conditions caused by uncertainty through additional information input. For load forecast error type of events, it is necessary to reschedule by updating the forecast value, and for unit maintenance type of events, the unit commissioning status and power output limit within the model are adjusted. Intraday scheduling is effective in coping with stochastic events with long time scale impacts (hourly level or more) and improves flexibility compared to the day-ahead scheduling model.

III. C. Validation of the effectiveness of the improved adaptive genetic algorithm

III. C. 1) Test Function Validation

After analyzing the integrated energy system algorithm, it is necessary to verify the effectiveness of the IFWA-SFLA algorithm, and three typical functions in Benchmark function: Ackley function, Rastrigin function and Griewank function are selected as the test functions to simulate and test the proposed algorithm, and the specific information of the above three functions is as follows:

(1) Ackley function

$$f_1(x) = -20 \times e^{-0.2 \times \sqrt{\frac{1}{n}\sum_{i=1}^{n} x_i^2}} - e^{\frac{1}{n}\sum_{i=1}^{n} \cos(2\pi x_i)} + 22.71282 \quad x_i \in [-10,10] \tag{27}$$

The image of this function is shown in Figure 5. The Ackley function is an almost flat region with a hole or peak formed by a cosine wave modulation, resulting in an undulating surface with a large hole in the center. The function has multiple local optima in the definition domain $\{x_i \in [-10,10], i = 1,2,\cdots,n\}$, but there is only one minimum value $f_{1,\min} = 0$ when the function is located at (0,0,...,0), which leads to the algorithm being very prone to optimization process fall into the local optimum, and the search for optimal larger regions in order to cross the valley of interference, and gradually reach a better optimal value.

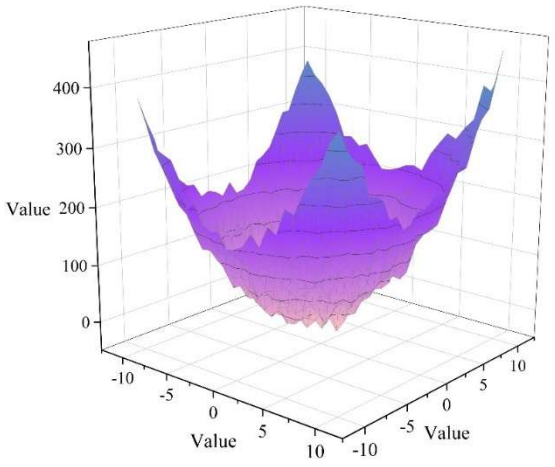

Figure 5: Ackley function image

(2) Rastrigin function

$$f_2(x) = \sum_{j=1}^{s} \left[x_j^2 - 10\cos(2\pi x_j) + 10 \right] x_j \in [-5,5] \tag{28}$$

The Rastrigin function is a nonlinear multi-peak function and the image of this function is shown in Fig. 6. The function has uneven heights and peak shapes with jumps, and there are 10^s local minima in the domain of definition $\{x_j \in [-5,5], j = 1,2,\cdots,n\}$, and the distribution of the local minima is scattered in the range of $(x_1, x_2, ..., x_i) = (0,0,...,0)$ at the unique minimum value $f_{2,\min} = 0$.

(3) Griewank function

$$f_3(x) = \sum_{k=1}^{d} \frac{x_k^2}{4000} - \prod_{k=1}^{d} \cos\left(\frac{x_k}{\sqrt{i}} r\right) + 1 \quad x_k \in [-600,600] \tag{29}$$

Griewank function is a nonlinear multimodal function the function image is shown in Figure 7. There are multiple local minima in the domain of definition, and the number of local minima is related to the function dimension. As the function dimension increases, the Griewank function appears to be difficult to optimize during the optimization

process, and the optimization difficulty is difficult before it is easy, and only in the case of $(x_1, x_2, ..., x_i) = (0, 0, ..., 0)$ at which there exists a unique minimum value $f_{3.\min} = 0$.

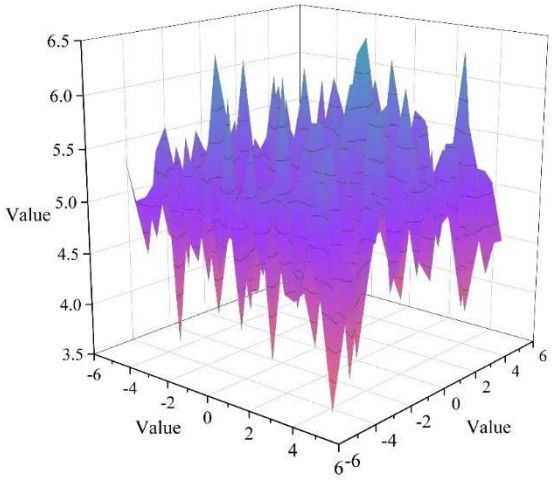

Figure 6: Rastrigin function image

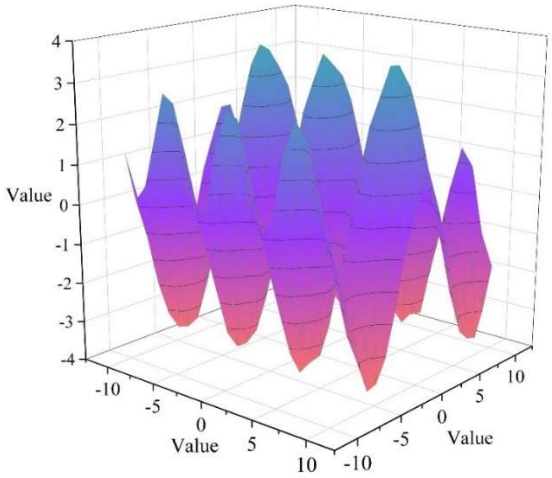

Figure 7: Griewank function image

The parameter settings of the improved GA algorithm in this paper are shown in Table 4, and the GA algorithm and SFLA algorithm solve the Ackley function, the Rastrigin function and the Griewank function respectively, and the global optimal solution and the average value of the optimal solution are shown in Table 5. Table 5 shows that for the three high-dimensional nonlinear functions, the global optimal solution and the average value of the optimal solution of the improved adaptive genetic algorithm proposed in this paper are better than the other two algorithms, and it has better convergence accuracy.

Table 4: Parameter setting of three algorithms

GA and improved GA algorithm parameter Settings		SFLA parameter setting	
Set name	Parameter	Set name	Parameter
Quantity of initial equipment	9	Population quantity	9
Initial generation	66	Quantity per population	66
Optimization problem dimension	18	Iteration times per population	27
Maximum iteration number	53	Maximum iteration number	53

Table 5: Comparison of optimization results of three algorithms

Test function	Optimization algorithm	Global optimal solution	Optimal average	The optimal solution of the function theory
Ackley	GA	0.9443	1.0266	0
	SFLA	0.2003	0.2616	
	Improvement GA	0.0808	0.1373	
Rastrigin	GA	1.1567	1.8959	0
	SFLA	0.5383	1.0127	
	Improvement GA	0.0985	0.1892	
Griewank	GA	0.7643	0.9923	0
	SFLA	0.7463	0.7823	
	Improvement GA	0.0643	0.4123	

The iteration curves obtained from the solution are shown in Fig. 8, Fig. 9 and Fig. 10. From Figures 8, 9 and 10, it can be seen that the three algorithms are able to solve the three Benchmark function global optimal solutions after several iterations, but there are differences in the iteration accuracy and convergence speed: GA reaches the global optimal solution after about 34, 28 and 41 iterations, but it is obviously trapped in the local optimal solution, which leads to an over-sized result; SFLA reaches the global optimal solution after about 49, 69 and 59 iterations, and the solution accuracy is obviously higher than GA; the proposed algorithm in this paper first uses GA to solve for the global optimal solution, which is significantly better than GA. After 49, 69 and 59 iterations, SFLA is near the global optimum, and the solution accuracy is significantly higher than that of GA. The algorithm proposed in this paper firstly adopts GA for global optimization, and then switches to SFLA for the 32nd, 35th and 44th iterations for the three test functions, respectively, to continue optimization, and then iterates for the Ackley function for 12 times to find the final optimal solution, and then iterates for the Rastrigin function for 10 times to find the final optimal solution, and then iterates for the Rastrigin function for 10 times to find the final optimal solution. The total number of iterations is less than that of SFLA, because the Gaussian variant of GA is changed to levy variant, which enhances the diversity of the optimization objects and avoids falling into the local optimum, and makes the algorithm's optimal solution in the global range more accurate.

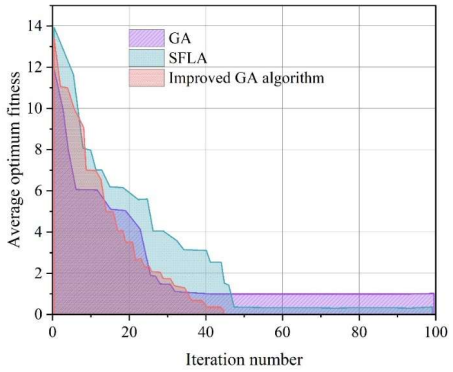

Figure 8: Ackley function iteration curve

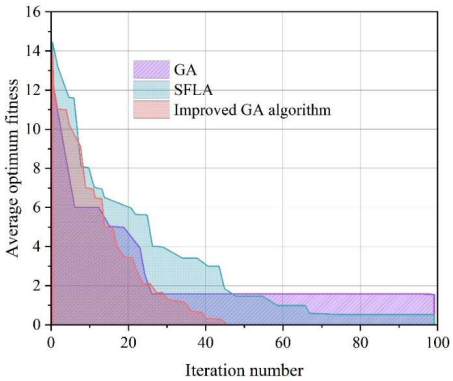

Figure 9: Rastrigin function iteration curve

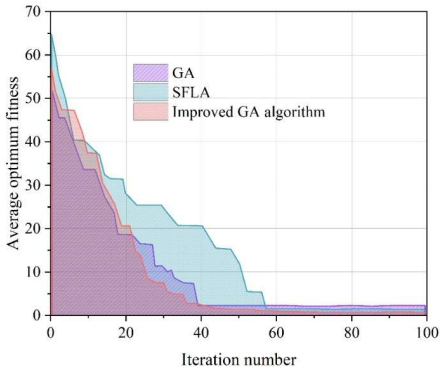

Figure 10: Griewank function iteration curve

The above results for the three test functions show that the improved adaptive genetic algorithm proposed in this paper outperforms both GA and SFLA in terms of the efficiency of solving the optimal solution, and the mixing of the two algorithms takes into account the convergence speed and accuracy.

III. C. 2) Validation of operational cost effectiveness

In order to verify the effectiveness of the improved adaptive genetic algorithm in optimizing the operating cost of the integrated energy system, PSO, GA and SFLA are selected as comparison algorithms, and the optimal value of the cost is optimally calculated for 100 times. The results of the algorithm calculations are shown in Table 6 and Table 7, and the algorithm iteration diagrams are shown in Figure 11 and Figure 12.

From Table 6 and Fig. 11, it can be seen that in the day-ahead scheduling optimization calculation, the optimal cost of the improved GA algorithm and the traditional GA algorithm is lower than that of the PSO algorithm, which indicates that the convergence speed and global optimization search efficiency of the traditional GA algorithm are better than that of the PSO algorithm. The traditional GA algorithm converges fast in the pre iteration period and converges near the global optimum in 46 iterations, but the optimal value found in the later period is higher.SFLA converges to the optimal value in 61 iterations, and the cost has the most value than the traditional GA algorithm, but the number of iterations is too many and the computation time is longer. The improved GA algorithm first uses IFWA to find the neighborhood of the optimal value, switches to SFLA at 54 iterations, and continues the local optimization search to find the global optimal value of 53,295 yuan, which is better than the other three algorithms, and the number of iterations is smaller than PSO and SFLA.

In Table 7 and Fig. 12 intraday scheduling optimization calculations, the superiority of the algorithm proposed in this paper is similar to that of the other day, which fully demonstrates the effectiveness of IFWA-SFLA in the optimized scheduling of integrated energy systems.

Table 6: Day-ahead calculation results of algorithms

Algorithm	Global optimal value/yuan	Buy electric bills/yuan	Buy electric bills/yuan	The number of times before
PSO	56154	28354	29438	73
GA	55971	27873	29323	49
SFLA	53959	25978	28256	65
Improved GA algorithm	53777	24592	26958	55

Table 7: Intraday calculation results of algorithms

Algorithm	Global optimal value/yuan	Buy electric bills/yuan	Buy electric bills/yuan	The number of times before
PSO	55151	25358	30301	70
GA	54977	24675	30463	49
SFLA	52759	23730	28858	61
Improved GA algorithm	52378	22136	28048	50

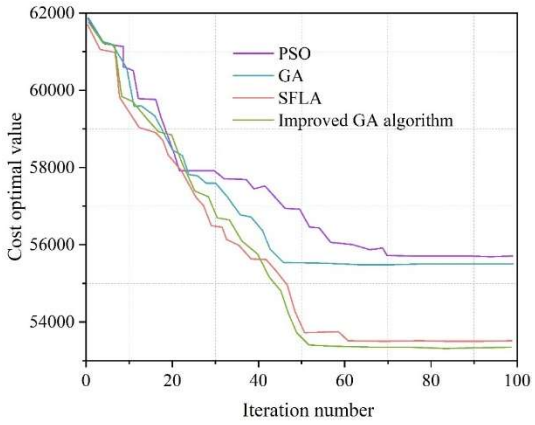

Figure 11: Iterative graph of algorithm day-ahead scheduling

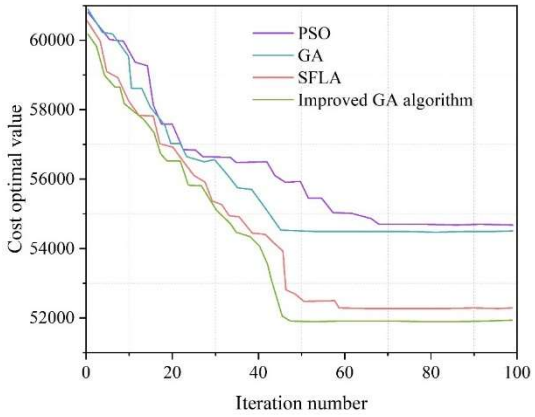

Figure 12: Iterative graph of algorithm intraday scheduling

IV. Conclusion

In this paper, we propose a multi-timescale integrated energy system scheduling model considering combined thermal and electrical flexible loads, and adaptively adjust the crossover probability and variance probability of the genetic algorithm based on the individual's fitness in the population. The following conclusions are drawn from the research results:

(1) Intraday scheduling can effectively avoid the influence generated by load forecast deviation and load fluctuation time, reduce the system's energy supply cost and energy supply reliability, and improve the energy supply cost of control system operation.

(2) By selecting three Benchmark functions such as Ackley function, Rastrigin function and Griewank function, and comparing and analyzing them with the traditional GA algorithm and SFLA to verify the effectiveness of the improved adaptive genetic algorithm, the results show that the algorithm proposed in this paper takes into account of both the optimization accuracy and optimization speed, and it can be well adapted to accurately solve the nonlinear model.

Funding

This work was supported by Science and Technology Project of Zhejiang Dayou Group Co., Ltd. (DY2024-11).

References

[1] Tuballa, M. L., & Abundo, M. L. (2016). A review of the development of Smart Grid technologies. Renewable and Sustainable Energy Reviews, 59, 710-725.

[2] Dileep, G. J. R. E. (2020). A survey on smart grid technologies and applications. Renewable energy, 146, 2589-2625.

[3] Yang, X., He, H., Zhang, Y., Chen, Y., & Weng, G. (2019). Interactive energy management for enhancing power balances in multi-microgrids. IEEE Transactions on Smart Grid, 10(6), 6055-6069.

[4] Yang, J. Y., Song, Y. H., & Kook, K. S. (2024). Critical Inertia Calculation Method of Generators Using Energy Balance Condition in Power System. Energies, 17(5), 1097.

[5] Ding, L., Wang, J., Ru, W., Xu, Z., Sa, P., & Jiang, W. (2022, November). Electric Power Balance Contribution Calculation Based on Power Traceability. In International Joint Conference on Energy, Electrical and Power Engineering (pp. 447-456). Singapore: Springer Nature Singapore.
[6] Puzakov, A. (2021). Estimation of efficiency of electric power balance iautomobiles. Transport Problems, 16(2), 113-120.
[7] Saukh, S. (2020, October). The Balance of Power Differentials and Its Application for the Analysis of Electric Power Systems. In 2020 IEEE 2nd International Conference on System Analysis & Intelligent Computing (SAIC) (pp. 1-5). IEEE.
[8] Goncharov, V. D., & Yashkardin, R. V. (2021). A Method for Calculating the Balance of Energy Released in Elements of High-Power Pulse Installations. Russian Electrical Engineering, 92(3), 159-162.
[9] Petrushyn, V., Horoshko, V., Plotkin, J., Almuratova, N., & Toigozhinova, Z. (2021). Power balance and power factors of distorted electrical systems and variable speed asynchronous electric drives. Electronics, 10(14), 1676.
[10] Ageev, V. A., Dushutin, K. A., Repyev, D. S., Kazakov, D. V., Volgushev, P. A., & Burnaev, A. I. (2021, March). Approach to composition of power balance of electric networks. In 2021 3rd International Youth Conference on Radio Electronics, Electrical and Power Engineering (REEPE) (pp. 1-4). IEEE.
[11] Cremer, J. L., Konstantelos, I., Tindemans, S. H., & Strbac, G. (2018). Data-driven power system operation: Exploring the balance between cost and risk. IEEE Transactions on Power Systems, 34(1), 791-801.
[12] Silwal, B., Rasilo, P., Perkkiö, L., Hannukainen, A., Eirola, T., & Arkkio, A. (2015). Numerical analysis of the power balance of an electrical machine with rotor eccentricity. IEEE Transactions on Magnetics, 52(3), 1-4.
[13] Hattori, S., Eto, H., Kurokawa, F., & Kajiwara, K. (2018). An evaluation of charging power balance of EV battery for household distributed power system. International Journal of Renewable Energy Research, 8(1), 1-6.
[14] Kamnarn, U., Yodwong, J., Piyawongwisal, P., Wutthiwai, P., Namin, A., Thounthong, P., & Takorabet, N. (2022). Design and simulation of DC distributed power supply with power balance control technique. International Journal of Power Electronics and Drive Systems (IJPEDS), 13(1), 460-469.
[15] Chen, Y., Lu, Q., Zhang, Z., Xu, T., Yang, Y., & Liu, Y. (2023, March). A medium/long-term electrical power and electrical energy balance method for power system considering extreme weather. In 2023 5th Asia Energy and Electrical Engineering Symposium (AEEES) (pp. 749-752). IEEE.
[16] Shafi, I. C. (2023). BALANCE OF ELECTRICAL ENERGY IN ELECTRICAL NETWORKS AND COMMERCIAL LOSS ANALYSIS. German International Journal of Modern Science/Deutsche Internationale Zeitschrift für Zeitgenössische Wissenschaft, (64).
[17] Reymov, K. M., Rafikova, G. R., & Esemuratova, S. (2020). Existing condition and prospects of making power balance and managing load of electric consumers in uzbek power system. In E3S web of conferences (Vol. 209, p. 07015). EDP Sciences.
[18] Sun, J., Mori, Y., & Nakade, K. (2018). A study of total optimisation model for supply balance in electric power market network. Asian Journal of Management Science and Applications, 3(4), 340-352.
[19] P.M. Sutheesh,Nagendra Reddy Bandi & Rohinikumar Bandaru. (2025). Thermal performance of Lithium-Ion battery pack with optimised bionic channel using Multi-Objective genetic Algorithm: A numerical Investigation. Thermal Science and Engineering Progress,60,103414-103414.
[20] Kapil Choudhary,Girish Kumar Jha,Ronit Jaiswal & Rajeev Ranjan Kumar. (2025). A genetic algorithm optimized hybrid model for agricultural price forecasting based on VMD and LSTM network. Scientific Reports,15(1),9932-9932.